Clipped random wave analysis of anisometric lamellar microemulsions

Dawen Choy[1] and Sow-Hsin Chen[2,*]
[1]*Department of Physics, Massachusetts Institute of Technology, Cambridge, Massachusetts 02139*
[2]*Department of Nuclear Engineering, Massachusetts Institute of Technology, Cambridge, Massachusetts 02139*
(Received 28 May 2000; published 10 January 2001)

Small-angle neutron scattering experiments were performed on $C_{10}E_4$-D_2O-octane (where $C_{10}E_4$ is tetraethylene glycol monodecyl ether) anisometric microemulsions in the lamellar phase at a constant surfactant volume fraction of 20% and at the hydrophile-lipophile balance temperature of 22.5 °C. The results were analyzed using a clipped random wave model with a specific spectral distribution function developed by us previously. This enabled us to generate three-dimensional morphologies of the microemulsions, which showed clearly that in sufficiently anisometric microemulsions the oil-water interface was no longer connected. At large anisometry isolated regions of oil or water were found, and the transition from a bicontinuous structure at isometry to these isolated micelles far from isometry goes through an intermediate cylindrical morphology when the oil-to-water or water-to-oil ratio is around 4 to 1. We further computed the joint distribution function of the mean curvature H and Gaussian curvature K of the entire oil-water interface for each anisometric microemulsion. In particular, we show the distribution of $\langle H\rangle$, $\langle K\rangle$, and $\langle H^2\rangle-\langle H\rangle^2$ for different isolated regions within an oil-rich microemulsion at an oil-to-water ratio of 85% to 15%. These distributions allowed us to prove that the isolated regions formed in highly anisometric microemulsions were small and had spherical topology.

DOI: 10.1103/PhysRevE.63.021401 PACS number(s): 82.70.−y

I. INTRODUCTION

Microemulsions are amphiphilic solutions containing oil, water, and surfactant which appear macroscopically miscible but in reality are phase separated on a microscopic scale, with the oil and water domains held in contact by the surfactant molecules. Depending on external parameters such as temperature and the relative volume ratios of oil, water, and surfactant, they exhibit a rich variety of internal structures including globular micelles, disordered bicontinuous membranes, and stacked lamellar planes.

As we showed in an earlier paper [1], dilute isometric lamellar microemulsions (containing equal proportions of water and oil) near the sponge-lamellar transition have a structure that is very similar to the disordered bicontinuous phase, marked by numerous passage defects [2]. It was therefore interesting to consider what happens in dilute anisometric lamellar microemulsions, where the imbalanced oil-to-water ratio causes the oil-water interface to curve significantly (toward water in oil-rich microemulsions, and vice versa) even at the hydrophile-lipophile balanced temperature. If the curvature becomes extreme enough, it is possible that the bicontinuous structure may break up into distinct, isolated regions.

To investigate the exact topological changes that accompany increasing anisometry, we performed small-angle neutron scattering experiments on $C_{10}E_4$-D_2O-octane microemulsions in the dilute lamellar phase ($C_{10}E_4$ represents tetraethylene glycol monodecyl ether). The clipped random wave model was then used to analyze the scattering results, from which three dimensional pictures of the microemulsion morphology were constructed. This allowed us to visualize the topological changes taking place in the microemulsion structure, from which it became clear that isolated water-in-oil or oil-in-water micelles were forming in highly anisometric microemulsions. Furthermore, by computing the distributions of the mean curvature and Gaussian curvature for the oil-water interface, we were able to prove that these isolated regions have spherical topology (with no holes in them).

II. CLIPPED RANDOM WAVE MODEL

In the clipped random wave (CRW) model [3], the order parameter field of a microemulsion system is first expanded in a series of spherically symmetric cosine waves with the magnitude of wave vectors $\mathbf{k}_n$ (isotropically distributed) chosen from a spectral distribution function $f(k)$, and with random phases ϕ_n uniformly distributed within the interval $[0,2\pi)$,

$$\psi(\mathbf{r})=\sqrt{\frac{2}{N}}\sum_{1}^{N}\cos(\mathbf{k}_n\cdot\mathbf{r}+\phi_n). \tag{1}$$

The order parameter field is normalized in such a way that $\langle|\psi|^2\rangle=1$, where the average is taken over the random phases. Since the order parameter field is a sum over many independent cosine waves, the central limit theorem guarantees that $\psi(\mathbf{r})$ is a continuous Gaussian random field with a mean square amplitude of unity, namely,

$$P(\psi)=\frac{1}{\sqrt{2\pi}}\exp\left(-\frac{\psi^2}{2}\right). \tag{2}$$

In this paper, we have also chosen to use the spectral function [1]

$$f(k)=\beta f_1(k)+(1-\beta)f_{3/2}(k), \tag{3}$$

*Email address: sowhsin@mit.edu

where

$$f_1(k)=\frac{1}{(2\pi\sigma_k^2)^{3/2}}\exp\left(-\frac{k^2}{2\sigma_k^2}\right),$$

$$f_{3/2}(k)=\frac{8}{\pi^2}\frac{b^3(a^2+b^2)}{[k^4-2(a^2-b^2)k^2+(a^2+b^2)^2]^2}, \quad (4)$$

a, b, β, and σ_k being parameters to be determined experimentally. This spectral function was derived by maximization of an associated generalized entropy function [4], subjected to the constraint that the second and fourth moments of the spectral function be finite.

Since microemulsions are microphase separated with distinct oil and water domains, a continuous $\psi(\mathbf{r})$ distribution is not quite appropriate. In order to create a discrete order parameter field that correctly represents the microphase separation, we clip the order parameter at a level α determined by the relative volume fractions of each component, resulting in an oil-water interface that is mathematically defined as

$$\psi(\mathbf{r})=\alpha. \quad (5)$$

This clipping operation generates a two-level discrete field $\zeta(\mathbf{r})$ from the original, continuous field $\psi(\mathbf{r})$ by assigning $\zeta(\mathbf{r})=1$ (water region) when $\psi(\mathbf{r})\geq\alpha$, and $\zeta(\mathbf{r})=0$ (oil region) when $\psi(\mathbf{r})<\alpha$. Strictly speaking, $\zeta(\mathbf{r})$ is only correct for describing two-component systems. Fortunately, the surfactant used in our three-component microemulsion, tetraethylene glycol monodecyl ether has a hydrophilic head and a hydrophobic tail that are almost equally sized. Together with the fact that we were investigating dilute lamellar microemulsions, where the amount of surfactant is still small compared to the amount of oil and water present, we were able to treat our three-component microemulsion as an effective two-component system by partitioning half (the tail) of the surfactant into the oil region and the other half (the head) into the water region. Thus, for anisometric microemulsions in general, α can be derived from Eq. (2), yielding the relationship

$$\varphi_1=\frac{1}{2}\left[1-\mathrm{erf}\left(\frac{\alpha}{\sqrt{2}}\right)\right], \quad (6)$$

where φ_1 is the volume fraction of water and half of the surfactant.

The scattering properties of such a clipped random wave system can be calculated entirely from the spectral function $f(k)$. First, by taking its Fourier transform, the two-point correlation function $g(|\mathbf{r}_1-\mathbf{r}_2|)=\langle\psi(\mathbf{r}_1)\psi(\mathbf{r}_2)\rangle$ is obtained,

$$g(r)=\int_0^\infty\frac{\sin(kr)}{kr}4\pi k^2 f(k)\,dk. \quad (7)$$

The normalized Debye correlation function is then given by [5]

$$\Gamma(r)=1-\frac{1}{2\pi\varphi_1\varphi_2}\int_0^{\cos^{-1}[g(r)]}\exp\left(-\frac{\alpha^2}{1+\cos\theta}\right)d\theta, \quad (8)$$

where φ_1 and φ_2 are the respective volume fractions of the two pseudocomponents of the system. Using the fact that $\alpha=0$ for isometric microemulsions, we can greatly simplify the expression for $\Gamma(r)$ in that case, resulting in the expression

$$\Gamma(r)=\frac{2}{\pi}\sin^{-1}[g(r)]. \quad (9)$$

By knowing the Debye correlation function, the scattering intensity can be obtained from the relation [6]

$$I_{\mathrm{CRW}}(Q)=\langle\eta^2\rangle\int\frac{\sin(Qr)}{Qr}4\pi r^2\Gamma(r)dr, \quad (10)$$

where $\langle\eta^2\rangle=(\Delta\rho)^2\varphi_1\varphi_2$, $\Delta\rho$ being the difference between the scattering length densities of oil and water (contrast). In practice, $\langle\eta^2\rangle$ is usually calculated from

$$\langle\eta^2\rangle=\frac{1}{2\pi^2}\int_0^\infty Q^2 I_{\mathrm{data}}(Q)dQ \quad (11)$$

so that calibration errors in $I_{\mathrm{data}}(Q)$ can be eliminated. Thus, using Eq. (10) to fit experimentally obtained scattering curves, one can then determine the values of the parameters a, b, β, and σ_k, and thereby obtain the spectral function $f(k)$ of the microemulsion being studied.

III. SIMULATIONS OF THE MICROEMULSION MORPHOLOGY

A key advantage of the clipped random wave model is that, having experimentally determined the spectral function of a given microemulsion, $f(k)$ can be used in Eq. (1) to generate a three-dimensional snapshot of the clipped order parameter field describing the microemulsion. For the simulation, it is usually more convenient to recast Eq. (1) into the form [1]

$$\psi(\mathbf{r})=\mathrm{Re}\sum_{\mathbf{k}}\left(\frac{2\pi}{L}\right)^{3/2}\sqrt{6f(\mathbf{k})}A(\mathbf{k})e^{i\mathbf{k}\cdot\mathbf{r}+i\phi(\mathbf{k})}, \quad (12)$$

where the sum is taken over wave numbers rather than individual cosine waves. Equation (12) also brings out explicitly the importance of $f(k)$. The order parameter field so obtained can then be used to visualize the oil-water interface by plotting the isovalue surface defined by Eq. (5). This allows us to look at the oil-water interface directly rather than dealing with the abstract parameters a, b, β, and σ_k of the spectral function.

One can do even better by calculating the Gaussian and mean curvatures of the oil-water interface at every surface point, defined as

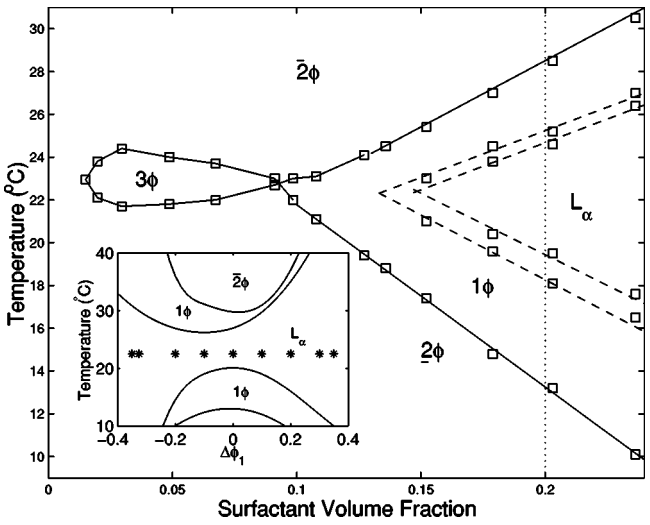

FIG. 1. Phase diagram of $C_{10}E_4$-D_2O-octane microemulsion on the isometric plane where the oil and water volume fractions are exactly equal. The inset shows a schematic diagram of the anisometric plane at $\varphi_s = 0.2$, where the asterisks denote the samples used for this experiment.

$$K = \frac{1}{R_1 R_2},$$

$$H = \frac{1}{2}\left(\frac{1}{R_1} + \frac{1}{R_2}\right), \tag{13}$$

where R_1 and R_2 are the principal radii at the surface point. Since the interface is mathematically defined by Eq. (5), the Gaussian and mean curvatures can be derived from the order parameter field using equations from differential geometry [7],

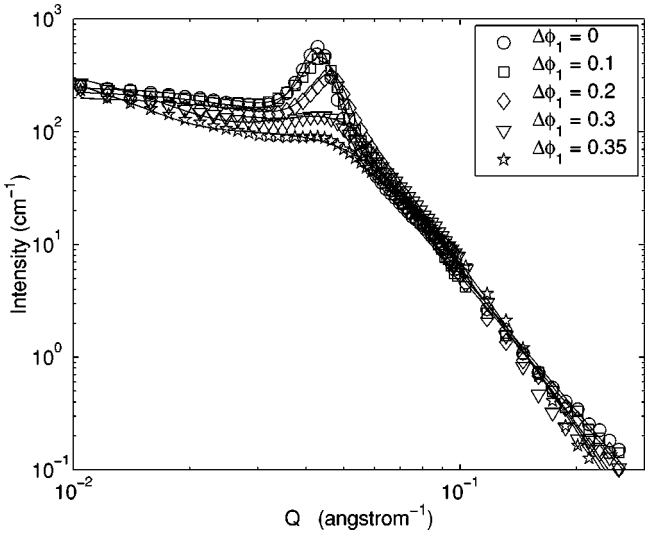

FIG. 2. Scattering intensity distributions (points) and CRW fits (solid lines) for $C_{10}E_4$-D_2O-octane isometric and water-rich microemulsions.

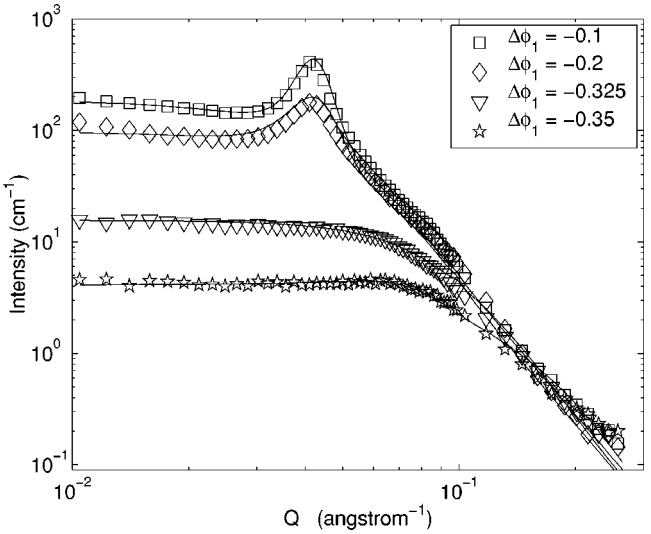

FIG. 3. Scattering intensity distributions (points) and CRW fits (solid lines) for $C_{10}E_4$-D_2O-octane oil-rich microemulsions.

$$K = \frac{1}{M^4}[\psi_{xx}\psi_{yy}\psi_z^2 - \psi_{xy}^2\psi_z^2 + 2\psi_{xz}\psi_x \times (\psi_y\psi_{yz} - \psi_z\psi_{yy}) + \text{permutations}],$$

$$H = \frac{1}{2M^3}[\psi_{xx}(\psi_y^2 + \psi_z^2) - 2\psi_x\psi_y\psi_{xy} + \text{permutations}], \tag{14}$$

where ''permutations'' indicates additional terms obtained by cyclic permutation, and where

$$M = \sqrt{\psi_x^2 + \psi_y^2 + \psi_z^2}. \tag{15}$$

In previous studies of anisometric microemulsions [8] only average values of the Gaussian and mean curvatures, taken over the entire oil-water interface, were calculated. However, because the oil-water interface is not necessarily a single continuous surface in anisometric microemulsions, these average values become topologically meaningless. According to the Gauss-Bonnet theorem

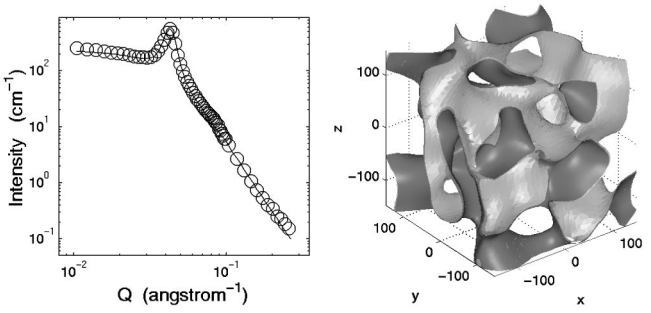

FIG. 4. Scattering intensity (circles) and CRW fit (line) of isometric microemulsion, together with a 3D picture of the microemulsion structure generated by computer simulation. Length scales for the simulation are in angstroms.

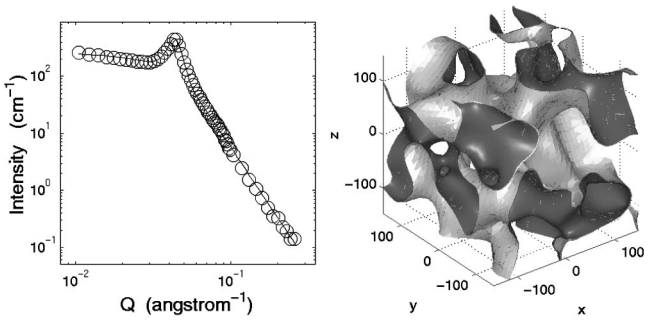

FIG. 5. Scattering intensity (circles) and CRW fit (line) of $\Delta\varphi_1=0.1$ microemulsion, together with a 3D picture of the microemulsion structure generated by computer simulation. Length scales for the simulation are in angstroms.

$$\langle K\rangle S=4\pi(1-n), \tag{16}$$

where S is the total surface area of a closed surface and n is the number of holes in it, the average Gaussian curvature $\langle K\rangle$ is only useful when taken over a *closed* surface. Thus, the ability to calculate the surface distribution of K and H, given by Eq. (14), is crucial to the analysis of anisometric microemulsions.

Coupled with an algorithm that locates individual closed surfaces within a simulated order parameter field, the clipped random wave model provides a very powerful tool for analyzing anisometric microemulsions. One can study the formation of isolated regions of oil or water as the microemulsion departs from isometry, and even track any changes in topology by calculating $\langle K\rangle$ for each closed surface.

IV. EXPERIMENTS

Small-angle neutron scattering experiments were performed on $C_{10}E_4$-D_2O-octane anisometric microemulsions in the lamellar phase. These experiments were carried out using time-of-flight spectroscopy on the SAND instrument of the Intense Pulsed Neutron Source (IPNS) at Argonne National Laboratory. The surfactant volume fraction was kept at 20% for all the samples studied, and the temperature was maintained at 22.5 °C. In order to differentiate between different anisometric microemulsions, the deviation of the microemulsion's water volume fraction from the isometric case of 0.5 was used, that is,

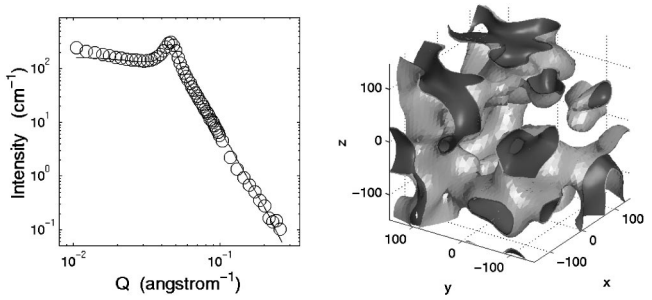

FIG. 6. Scattering intensity (circles) and CRW fit (line) of $\Delta\varphi_1=0.2$ microemulsion, together with a 3D picture of the microemulsion structure generated by computer simulation. Length scales for the simulation are in angstroms.

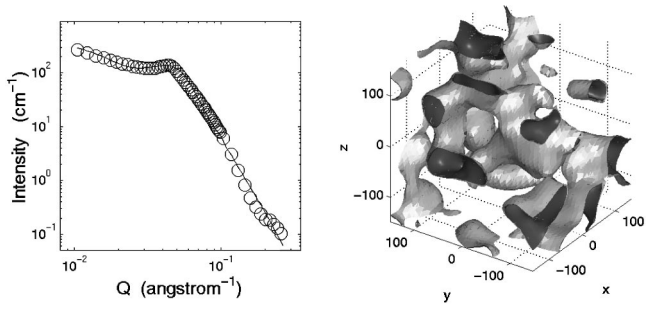

FIG. 7. Scattering intensity (circles) and CRW fit (line) of $\Delta\varphi_1=0.3$ microemulsion, together with a 3D picture of the microemulsion structure generated by computer simulation. Length scales for the simulation are in angstroms.

$$\Delta\varphi_1=\varphi_1-\frac{1}{2}, \tag{17}$$

where φ_1 is the volume fraction of the water component in the microemulsion. Note that, since we have partitioned half of the surfactant volume into the pseudowater component, φ_1 includes the volume fraction of both water and half the surfactant. Thus, a microemulsion with $\Delta\varphi_1=0.2$ is made up of 60% D_2O, 20% octane, and 20% $C_{10}E_4$ surfactant. Naturally, positive values of $\Delta\varphi_1$ indicate water-rich microemulsions, while negative values indicate oil-rich microemulsions. As can be seen from the phase diagram in Fig. 1, the experimental samples ranged from $\Delta\varphi_1=-0.35$ to $\Delta\varphi_1=0.35$.

We then analyzed the scattering results using the CRW model. The background due to incoherent scattering was first subtracted from the raw data. Furthermore, to correct for smearing due to resolution limitations of the SAND instrument, the theoretical scattering intensity was convolved with a Gaussian resolution function [9] before fitting to the experimental scattering distribution (see the Appendix). Using Eqs. (7), (8), and (10) to fit the experimental data, we were thus able to obtain values for the parameters a, b, β, and σ_k for the spectral function $f(k)$ of each microemulsion. The scattering data and their fitted curves are shown in Figs. 2

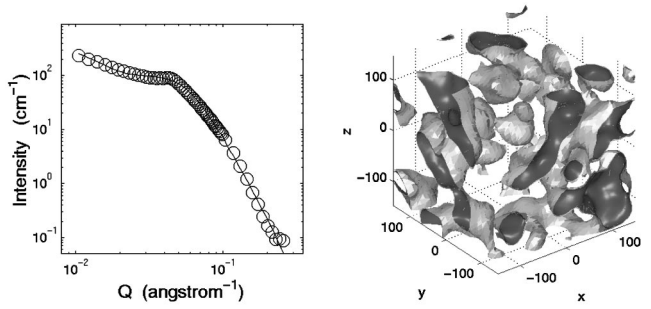

FIG. 8. Scattering intensity (circles) and CRW fit (line) of $\Delta\varphi_1=0.35$ microemulsion, together with a 3D picture of the microemulsion structure generated by computer simulation. Length scales for the simulation are in angstroms.

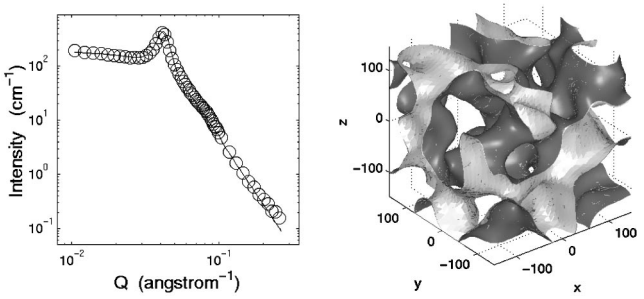

FIG. 9. Scattering intensity (circles) and CRW fit (line) of $\Delta\varphi_1 = -0.1$ microemulsion, together with a 3D picture of the microemulsion structure generated by computer simulation. Length scales for the simulation are in angstroms.

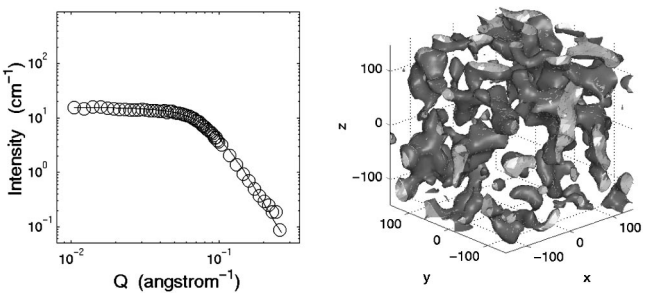

FIG. 11. Scattering intensity (circles) and CRW fit (line) of $\Delta\varphi_1 = -0.325$ microemulsion, together with a 3D picture of the microemulsion structure generated by computer simulation. Length scales for the simulation are in angstroms.

and 3 for water-rich and oil-rich microemulsions, respectively. These spectral functions were then used together with Eq. (12) to generate three-dimensional simulations of the microemulsion oil-water interface, allowing us to track changes in the interface as the oil-water ratio was varied.

V. RESULTS AND DISCUSSION

A. Structural changes to the oil-water interface

The results of the fitting and simulation process are shown in Figs. 4–12. The size of the simulated order parameter field was $75\times75\times75$ elements, with each element representing a real-space volume of $8\times8\times8$ Å^3.

From the scattering curves, it becomes apparent that, as a microemulsion deviates from isometry and becomes oil- or water-rich, the peak in its scattering distribution flattens; in extreme cases, the peak even disappears. In addition, the absolute scattering intensity decreases away from isometry because the contrast between the oil and water components is reduced as one of them dominates.

Looking at the corresponding three-dimensional (3D) simulations of the microemulsions, one also observes that the disordered, bicontinuous structure of the oil-water interface in an isometric microemulsion gives way to a more dispersed structure in a highly anisometric microemulsion. In Fig. 8, which shows a water-rich microemulsion containing 85% water and 15% oil, disconnected micelles of oil surrounded by water can be clearly seen. Micelles are also found in the oil-rich analog, shown in Fig. 12, although they are smaller and much more numerous than in the water-rich case. There also seems to be an intermediate stage where the oil-water interface adopts a somewhat cylindrical structure, which can be seen in Figs. 7 and 11.

As is apparent from the scattering distributions and the 3D simulations, there is also some asymmetry between oil-rich and water-rich microemulsions with the same degree of anisometry—the structural changes in the oil-water interface due to the increasing dominance of one component seem to occur faster in oil-rich microemulsions. For example, micelle formation is much more pronounced in the highly oil-rich sample ($\Delta\varphi_1 = -0.35$) than in the corresponding water-rich sample ($\Delta\varphi_1 = 0.35$). This asymmetry is not unexpected since water and oil have different chemical potentials in solution [10]. Furthermore, the octane molecule is much larger than the three-atom water molecule; thus the formation of small micelles is much easier in oil-rich microemulsions (water inside the micelle) than in water-rich microemulsions, as is observed.

B. Joint probability distribution of *K* and *H*

The clipped random wave model also allowed us to calculate the surface distribution of the Gaussian curvature *K* and the mean curvature *H*. From this surface distribution, we were able to construct the joint distribution of *K* and *H* over the oil-water interface, shown in Figs. 13 and 14. Both fig-

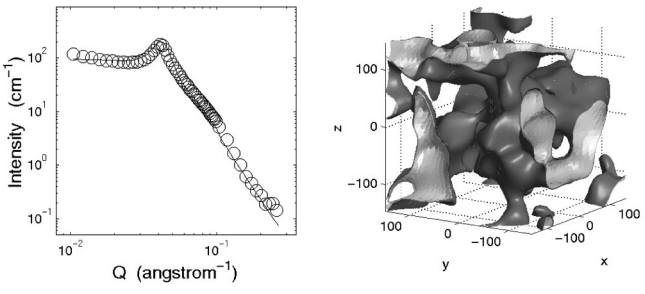

FIG. 10. Scattering intensity (circles) and CRW fit (line) of $\Delta\varphi_1 = -0.2$ microemulsion, together with a 3D picture of the microemulsion structure generated by computer simulation. Length scales for the simulation are in angstroms.

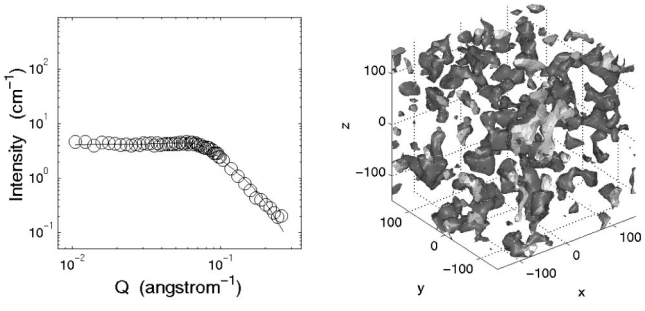

FIG. 12. Scattering intensity (circles) and CRW fit (line) of $\Delta\varphi_1 = -0.35$ microemulsion, together with a 3D picture of the microemulsion structure generated by computer simulation. Length scales for the simulation are in angstroms.

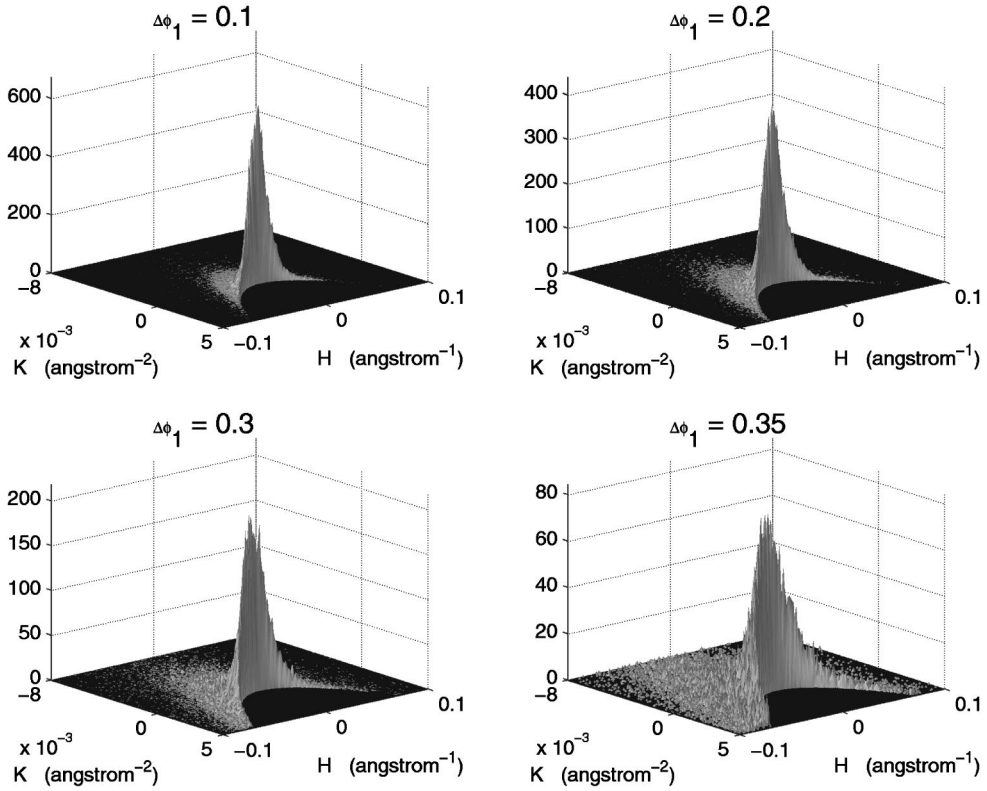

FIG. 13. Joint probability distributions of H and K for water-rich microemulsions. The plots shown are actually two-dimensional histograms of K, H pairs on the oil-water interface, so the vertical axis is accurate only up to a scale factor.

ures demonstrate that as the microemulsions become increasingly anisometric the spread of K and H values increases. More importantly, a greater proportion of surface elements begin to have positive K values, which is consistent with our earlier observation that the microemulsion begins to develop cylindrical and micellar structures.

C. Analysis of disconnected regions in highly anisometric microemulsions

The joint probability distribution of K and H, while very useful for a single continuous surface, becomes less significant when the oil-water interface is instead disconnected into many separate surfaces. This is especially so for the distribution of the Gaussian curvature K, because it is only topologically meaningful when taken over a single closed surface. In order to address this difficulty, we created a simple computer program to identify all disconnected regions of water or oil within the simulated order parameter field. Our algorithm looked for six-connected regions, and since the simulation is bounded we discarded isolated regions that were on the boundary as they may be ''connected'' outside the simulation boundary. After identification, we could then easily tabulate the size, $\langle K \rangle$, and $\langle H^2 \rangle$ (amongst others) of each disconnected region and its associated oil-water interface, allowing us to track the formation of these disconnected regions in highly anisometric microemulsions. This process would also allow us to check that the oil-water interface was in fact bicontinuous for microemulsions near isometry.

Our results indicate that, for microemulsions within $-0.2 < \Delta\varphi_1 < 0.2$, the oil-water interface is essentially bicontinuous. The program detected only 1–3 very small disconnected regions in the boundary cases of $\Delta\varphi_1 = \pm 0.2$, which could easily be discounted as mathematical artifacts of the simulation process. For more anisometric samples, however, the number of disconnected regions increased very quickly. Within an order parameter field of dimensions $600 \times 600 \times 600$ Å^3, one particular run of the simulation yielded 52 disconnected regions for the $\Delta\varphi_1 = 0.35$ sample, 138 for the $\Delta\varphi_1 = -0.325$ sample, and 499 for the $\Delta\varphi_1 = -0.35$ sample. Even if we discounted regions that were smaller than three volume elements in size, we still found 39, 87, and 295 disconnected regions, respectively. It is clear that micelle formation is taking place in these highly anisometric microemulsions.

Histograms for the size, $\langle K \rangle$, $\langle H \rangle$, and $\langle H^2 \rangle - \langle H \rangle^2$ distributions of the disconnected regions in a $\Delta\varphi_1 = -0.35$ microemulsion are shown in Figs. 15 and 16 as an example, and are typical of the plots obtained with other samples containing disconnected regions. In general, the observed regions are quite small, with most of them being smaller than 20 volume elements although there are some regions larger than 100 volume elements. This finding is probably the result of a relatively high surfactant volume fraction of 20%, so that small micelles with high surface-to-volume ratios are favored. It would be interesting to perform similar experiments for microemulsions with different surfactant volume fractions to see whether micelle size is indeed inversely corre-

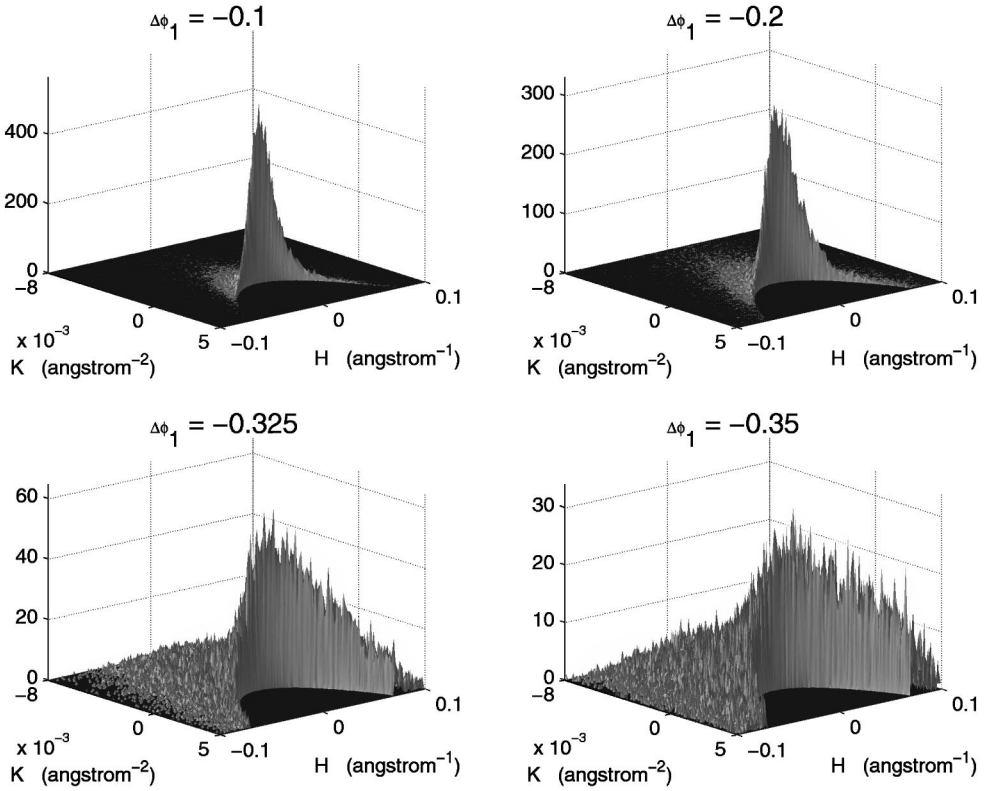

FIG. 14. Joint probability distributions of H and K for oil-rich microemulsions. The plots shown are actually two-dimensional histograms of K, H pairs on the oil-water interface, so the vertical axis is accurate only up to a scale factor.

lated, although that is beyond the scope of the present study.

The predominance of positive $\langle K \rangle$ values in Fig. 16 also indicates that these disconnected regions generally have a spherical topology with no holes in them. Furthermore, the values obtained are very high compared to the overall distribution of K across the entire oil-water interface within the microemulsion. Most of the disconnected regions have $\langle K \rangle$ greater than 0.01 Å^{-2}, whereas the majority of other surface points have values of K less than 0.005 Å^{-2}, as seen in Fig. 14. Using the definition of Gaussian curvature K in Eq. (13), the high values of $\langle K \rangle$ confirm that the regions are indeed very small.

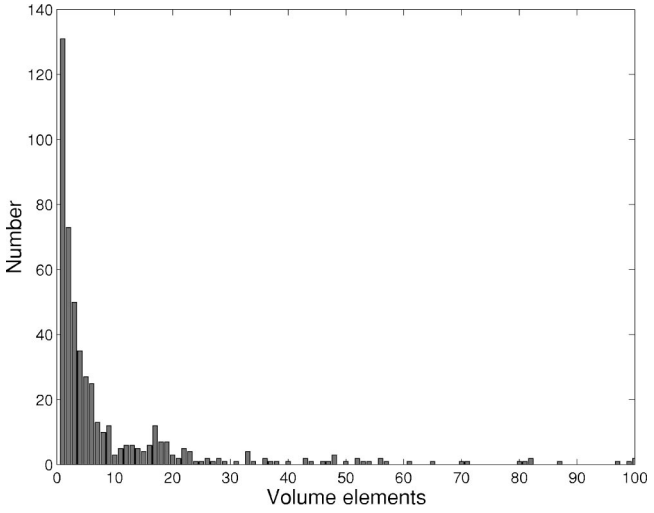

FIG. 15. Histogram of the volumes of disconnected regions found in a $\Delta\varphi_1 = -0.35$ microemulsion.

Fluctuations in the curvature of the oil-water interface surrounding these regions are generally small, as indicated by the relatively low variance of H shown. One should, however, discount the large number of regions with $\text{Var}(H) = 0$ as mathematical artifacts of the simulation, because these correspond to regions that are exactly the size of one volume element, in which case there is only a single value of H and $\text{Var}(H)$ is no longer meaningful.

It is also interesting to consider the remaining oil-water interface after subtracting away the disconnected regions, as shown in Fig. 17 . The surface is clearly cylindrical in shape with a rather open structure.

Our results therefore suggest the following changes in topology as a microemulsion departs from isometry, keeping the surfactant volume fraction constant. Take, for example, the case of an increasingly water-rich microemulsion. As the relative fraction of water begins to increase, the need to preserve the total amount of surfactant (due to constant surfactant fraction) forces the interface to adopt a cylindrical shape in order to increase the surface-to-oil volume ratio. The cylindrical structure becomes thinner and more open as the amount of oil is further decreased, until it becomes impossible to pack more surfactant molecules (of non-negligible size) onto the cylinder surface. Micelle formation is then necessary to increase the surface-to-oil volume ratio beyond that which is achievable by the connected cylindrical surface.

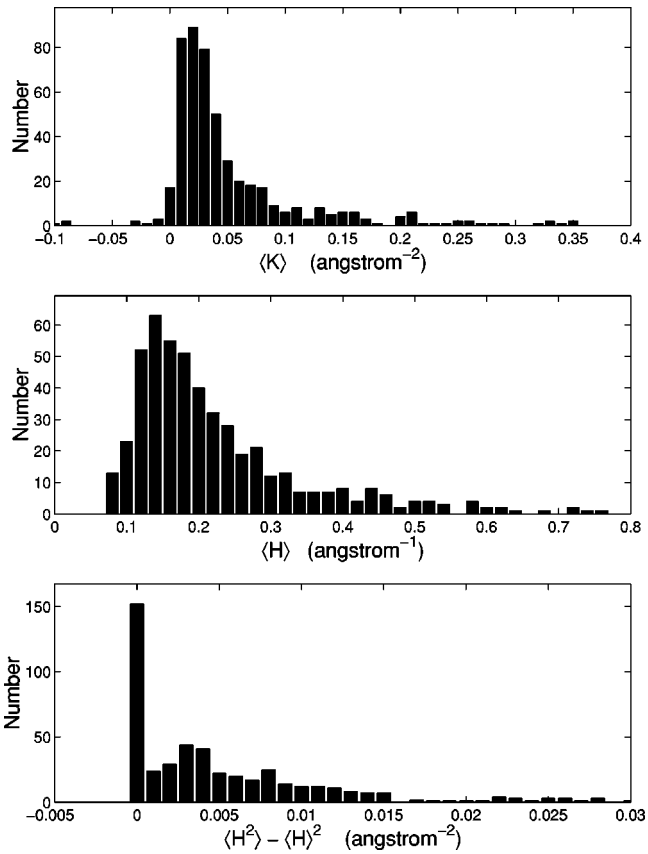

FIG. 16. Histograms of $\langle K \rangle$, $\langle H \rangle$, and Var(H) of the oil-water interface of these disconnected regions found in a $\Delta\varphi_1 = -0.35$ microemulsion.

VI. CONCLUSION

We have shown that the clipped random wave model is applicable to the analysis of the small-angle scattering intensity distribution of anisometric microemulsions (as well as isometric microemulsions [1]) at the hydrophile-lipophile balance temperature. The CRW model allows us to generate 3D morphologies of the oil-water interface consistent with the scattering intensity distribution, as well as compute the curvatures at each imaginary oil-water interface point. Thus, through these geometrical quantities, one can detect the topological transition as the water-to-oil ratio is varied.

Up to about $\Delta\varphi_1 = \pm 0.2$, our results show that the oil-water interface is still connected within the simulation box size of $600 \times 600 \times 600$ Å^3. As the degree of anisometry is further raised, the morphology becomes increasingly cylindrical, and the cross section of the cylindrical structure becomes narrower and narrower until, when sufficiently far from isometry, isolated regions of oil or water begin to form. This occurs approximately when $\Delta\varphi_1$ exceeds ± 0.3, whereupon the interface starts to become disconnected and isolated pieces are detected within the simulation box. By detecting and analyzing these isolated regions separately, we have

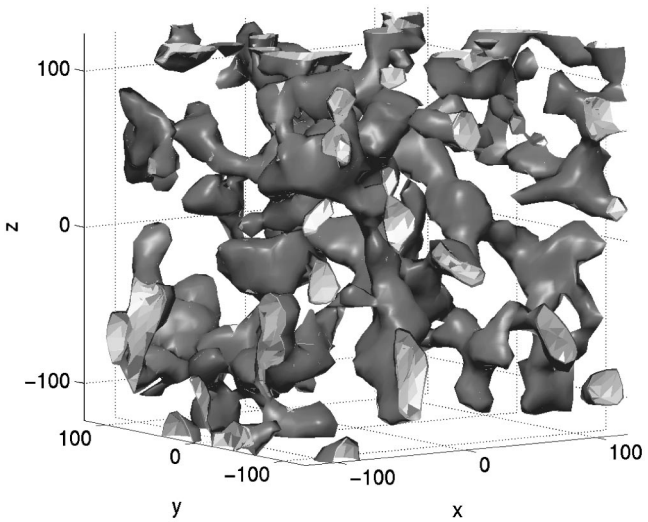

FIG. 17. 3D picture of $\Delta\varphi_1 = -0.35$ microemulsion after discarding the disconnected regions. The remaining oil-water interface is distinctly cylindrical. Length scales shown are in angstroms.

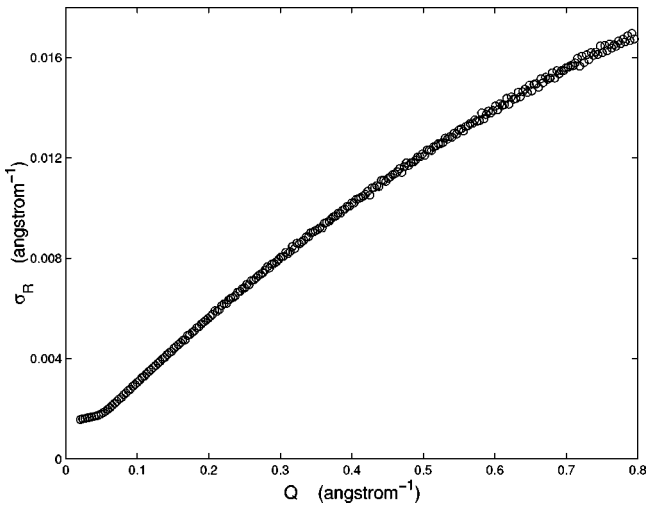

FIG. 18. Width of SAND resolution function.

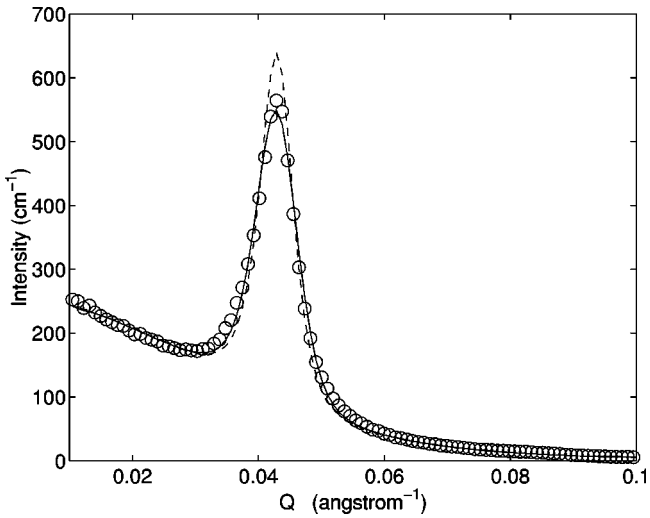

FIG. 19. Experimental scattering intensity (circles) of the $\Delta\varphi_1 = 0$ sample with the CRW fit before correction (dashed) and after correction (solid).

proved that they are relatively small and have spherical topology, with $\langle K \rangle > 0$. Thus, even though macroscopically the anisometric microemulsions we studied appeared to be in the lamellar phase, our analysis of their microscopic structure by neutron scattering suggests that the morphology is instead largely composed of an open cylindrical network together with isolated micelles.

ACKNOWLEDGMENTS

We would like to thank the instrument scientists at SAND, P. Thiyagarajan, K. C. Littrell, and D. G. Wozniak, for their help during our experiments. This research was supported by the Materials Chemistry Program of the Basic Energy Science division, U.S. Department of Energy.

APPENDIX: RESOLUTION CORRECTION

In this experiment, resolution effects were considered because we were dealing with microemulsions in the lamellar state that could potentially have very sharp scattering peaks. This was accomplished by convolving the theoretical scattering intensity obtained from the CRW model with a Gaussian resolution function,

$$I_{\mathrm{fit}}(Q) = \int_0^\infty \frac{I_{\mathrm{CRW}}(Z)}{\sqrt{2\pi\sigma_R^2}} \exp\left(-\frac{(Q-Z)^2}{2\sigma_R^2} \right) dZ, \qquad \text{(A1)}$$

where σ_R is the width of the resolution function. Data for σ_R were provided by the instrument scientists at SAND, and its variation with Q is shown in Fig. 18.

We then used this ''smeared'' intensity distribution to fit the experimental scattering curve. As Fig. 19 shows, resolution correction is quite important in getting an accurate fit to the experimental data, especially for microemulsions near isometry where the scattering peak is quite sharp.

[1] D. Choy and S. H. Chen, Phys. Rev. E **61**, 4148 (2000).

[2] As used in this context, ''dilute'' is not an exact definition tied to a specific range of surfactant volume ratios. Rather, it is used generally to define lamellar microemulsions whose surfactant volume ratio is not sufficient to generate the usual stacked lamellar structure. As discussed in our earlier paper [1], the stacked lamellar structure is typically maintained by Helfrich steric repulsions that decay with increasing distance between lamellar sheets. When this lamellar repeating distance is increased sufficiently that the Helfrich interaction is weak, thermal fluctuations will be strong enough to create topological defects in the stacked lamellar structure, leading to the disordered phase observed. At present, there is no theoretical means of deriving the point at which this breakdown in structure occurs, so for now we are confined to using ''dilute'' as an operational definition.

[3] N. F. Berk, Phys. Rev. Lett. **58**, 2718 (1987).

[4] C. Tsallis, J. Stat. Phys. **52**, 479 (1988); E. M. F. Curado and C. Tsallis, J. Phys. A **24**, L69 (1991).

[5] N. F. Berk, Phys. Rev. A **44**, 5069 (1991).

[6] P. Debye, H. R. Anderson, Jr. and H. Brumberger, J. Appl. Phys. **28**, 679 (1957).

[7] S. Hyde, *The Language of Shape: The Role of Curvature in Condensed Matter—Physics, Chemistry and Biology*, (Elsevier, Amsterdam, 1997).

[8] S. M. Choi, P. LoNostro, and S. H. Chen, Prog. Colloid Polym. Sci. **112**, 98 (1999).

[9] Values for the Q width of the resolution function were obtained from IPNS.

[10] M. C. Barbosa and M. Frichembruder, Phys. Rev. E **51**, 4690 (1995).